Performance of FBK high-density SiPM technology coupled to Ce:LYSO and Ce:GAGG for TOF-PET

2014 Phys. Med. Biol. 59 869

(http://iopscience.iop.org/0031-9155/59/4/869)

IOP Publishing | Institute of Physics and Engineering in Medicine Physics in Medicine and Biology

Phys. Med. Biol. **59** (2014) 869–880 doi:10.1088/0031-9155/59/4/869

Performance of FBK high-density SiPM technology coupled to Ce:LYSO and Ce:GAGG for TOF-PET

Alessandro Ferri, Alberto Gola, Nicola Serra, Alessandro Tarolli, Nicola Zorzi and Claudio Piemonte

Fondazione Bruno Kessler, via Sommarive 18, Trento, Italy

E-mail: aleferri@fbk.eu

Received 1 July 2013, revised 5 September 2013
Accepted for publication 18 December 2013
Published 3 February 2014

Abstract

This paper presents the performance, in terms of energy and timing resolution, of high-density silicon photomultipliers (SiPMs) produced at Fondazione Bruno Kessler for time-of-flight positron emission tomography application. The new SiPM technology allows us to produce devices with a small cell size maintaining a high fill factor (FF). The sensors considered in this paper are composed by $30 \times 30\ \mu m^2$ cells with a FF exceeding 70% to cover a total area of $4 \times 4\ mm^2$. The SiPM performance was evaluated using two types of scintillators (Ce:LYSO and Ce:GaGG) both with a short height (5 mm) in order to minimize the time jitter caused by light propagation in the crystal. With Ce:LYSO, an energy resolution of 9.0% FWHM at 511 keV and a coincidence resolving time (CRT) of 125 ps FWHM were obtained at $-20\ ^\circ C$. With Ce:GaGG, an energy resolution of 6.4% FWHM and a CRT of 260 ps FWHM were achieved at the same temperature. The novel SiPM technology, combining a high PDE with a low correlated noise (i.e., crosstalk and afterpulse), allows us to improve the state-of-the-art of energy and timing resolution with both the tested crystals.

Keywords: SiPM, LYSO, GaGG, PET, TOF

(Some figures may appear in colour only in the online journal)

1. Introduction

In the past few years Fondazione Bruno Kessler (FBK) has been involved in the development and optimization of silicon photomultipliers (SiPMs) for time-of-flight positron emission tomography (TOF-PET) application. One of the key design parameters of a SiPM is the cell size (CS). From geometrical considerations, for a given cell border technology, the smaller the

Table 1. Properties of the two scintillators used in this paper.

	Ce:LYSO	Ce:GaGG
Density (g cm^{-3})	7.1[a]	6.6[b]
Light yield (ph keV^{-1})	32[a]	46[b]
Decay time (ns)	40[a]	88[b]
Rise time (ps)	72[c]	200[d]
Intrinsic $\Delta E/E$ @ 662 keV (%)	7.1[a]	4.9[b]
Emission peak (nm)	420[a]	530[b]
Self radiation	Yes[a]	No[b]
Hygroscopicity	No[a]	No[b]

[a] Saint-Gobain (2012).
[b] Kamada *et al* (2011).
[c] Seifert *et al* (2012a).
[d] Yeom *et al* (2013b).

microcell size, the smaller the fill factor (FF). Thus, from the efficiency point of view, large cells are desirable. On the other hand, SiPMs with small microcells (e.g., CS $\leqslant$ 30 μm) have higher dynamic range, shorter recovery time, and less correlated noise (optical crosstalk and after-pulsing, both being proportional to the gain of the detector and thus the CS).

To reduce the CS not affecting the FF, or even improving it, a novel architecture of the cell border region has been developed. This new technology is called RGB-HD (Red Green Blue-High Density) and it is an evolution of the RGB one (Serra *et al* 2013). The implementation of trenches around the cells allowed a reduction of the dead border region from 7 to 2 μm. With this scheme two SiPMs were designed: a 2.2 $\times$ 2.2 mm^2 device with 15 $\times$ 15 μm^2 cells (described by Piemonte *et al* 2013), and a 4 $\times$ 4 mm^2 device with 30 $\times$ 30 μm^2 cells. The first SiPM has a FF of 48%, very similar to that of the 50 $\times$ 50 μm^2 cell of the RGB technology which was 45%, while the second has a FF of 75%. The total number of microcells is $\sim$21000 and $\sim$18000 for the 15 μm and 30 μm cells device, respectively.

In this paper, the functional properties as well as the performance evaluation for TOF-PET application of the first prototypes with 30 μm cells are presented. The SiPMs were tested for energy and timing resolution with two types of scintillator crystals, Ce:LYSO and Ce:GaGG, having the same size i.e., 3 $\times$ 3 $\times$ 5 mm^3. Although typical TOF-PET scanners use thicker crystals ($\sim$20 mm), the short configuration has been chosen to minimize the effect of time jitter due to light propagation. This scheme is widely used in literature to compare the SiPM performance. The main characteristics of the two scintillators are listed in table 1.

Cerium doped LYSO is the most widely used scintillator in PET application because of its properties: high density, high light yield, low decay time and absence of hygroscopicity. Many studies about this crystal coupled to SiPMs can be found in the literature. For example, Szczesniak *et al* (2011) measured 10.5% FWHM energy resolution at 511 keV with 5 $\times$ 5 $\times$ 5 mm^3 crystal coupled to a 2 $\times$ 2 matrix of 3 $\times$ 3 mm^2 MPPC (Multi Pixel Photon Counter, trade mark by Hamamatsu for SiPM), with 25 μm cells. Seifert *et al* (2012b) measured 138 ps FWHM coincidence resolving time (CRT) with a 3 $\times$ 3 $\times$ 5 mm^3 crystal coupled to a 3 $\times$ 3mm^2 MPPC with 50 μm cells. A CRT of 147 ps FWHM with the same crystal size and the same MPPC model was also reported by Yeom *et al* (2013a). Gola *et al* (2013) performed measurements with FBK initial SiPMs with 3 $\times$ 3 mm^2 active area and 69 μm cells coupled to 3 $\times$ 3 $\times$ 5 mm^3 LYSO, obtaining CRT of 186 ps FWHM at 20 °C and 158 ps FWHM at $-$20 °C. Finally, with the digital-SiPM by Philips, 10.7% FWHM energy resolution and 153 ps FWHM CRT with 3 $\times$ 3 $\times$ 5 mm^3 LYSO crystal have been reported (Haemisch *et al* 2012).

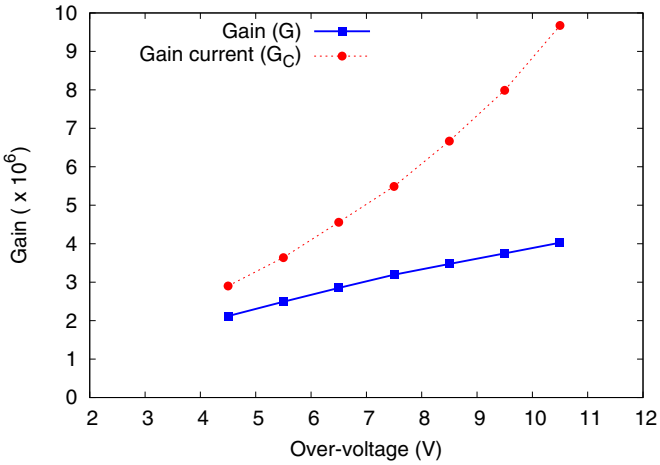

Figure 1. Measured gain and gain current as a function of the OV.

Cerium doped GaGG is a newly developed scintillator with interesting properties, especially the intrinsic energy resolution. There are only a few papers in the literature with studies on energy and timing performances for PET application of such material. Iwanowska *et al* (2013) measured energy and coincidence timing resolution of 10x10x5 mm^3 GaGG crystals coupled to PMTs, obtaining about 6.9% FWHM and 560 ps FWHM, respectively. They also coupled a $5 \times 5 \times 5$ mm^3 crystal to an 2×2 matrix of four 3×3 mm^2 Hamamatsu MPPCs with 25 μm CS and measured 7.2% FWHM energy resolution. In the same paper they estimated the crystal intrinsic resolution and found it to be about 6%, at 511 keV. Measurements with $3 \times 3 \times 5$ mm^3 crystals and 3×3 mm^2 MPPC with 50 μm cells have been reported (Yeom *et al* 2013b). The results were 7.9% FWHM energy resolution and 464 ps FWHM CRT. Kamada *et al* (2011) measured RGB SiPMs coupled to $3 \times 3 \times 5$ mm^3 GaGG crystal achieving 7.3% FWHM energy resolution and 286 ps FWHM CRT.

2. SiPM electro-optical characteristics

In this section, the main characteristics of the RGB-HD SiPM with 4×4 mm^2 active area and 30×30 μm^2 cells, are presented. The device testing procedure is described by Serra *et al* (2013) and Piemonte *et al* (2012). The measurements in dark conditions were carried out at -40 °C since at room temperature the noise events frequently pile up, altering the result. Nevertheless, from this measurements, it is possible to extract some device parameters, such as gain and correlated noise probability, that depend only on the over-voltage (OV) and not on the temperature.

Figure 1 shows the measured gain (G) as a function of the OV in blue squares. The gain is defined as the average charge produced by a single avalanche (excluding contribution from crosstalks and afterpulses), and can be calculated as the product of the cell capacitance times the OV. The gain of the RGB-HD SiPM is 3.0×10^6 and 3.6×10^6 at 7 and 9 V OV, respectively, which represent two typical operating conditions. Because of the incomplete depletion of the epitaxial layer at the breakdown voltage, at low OV the diode capacitance decreases with increasing bias, causing the nonlinear growth in the initial part. In fact, the cell capacitance extracted from G changes from 60 fF at 5 V OV to 45 fF at 9 V OV.

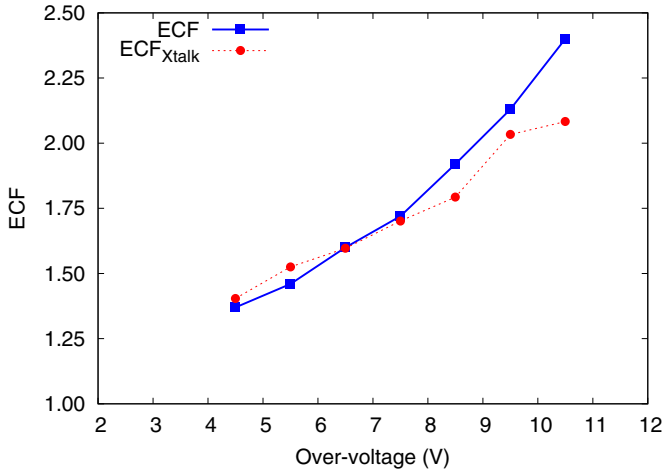

Figure 2. ECF as a function of the OV. ECF_{Xtalk} is the ECF calculated from the crosstalk probability only.

The gain current (G_C), reported in figure 1 in red circles, is defined as the average amount of charge carried by a primary event including contribution from crosstalks and afterpulses produced by that event. It can be calculated by dividing the dc reverse current by the primary dark count rate (DCR), as described in Piemonte *et al* (2013). The ratio G_C/G quantifies the amount of correlated noise in SiPMs, thus, it has been called excess charge factor (ECF). The ECF as a function of the OV is plotted in figure 2 (blue squares). It reaches 2 at about 9 V OV. The ECF can also be calculated from the direct measurements of the optical crosstalk and after-pulsing probabilities. Considering only the first phenomenon and approximating its development chain as a geometrical series, it can be estimated as:

$$\mathrm{ECF}_{X\mathrm{talk}} = 1/(1 - P_{X\mathrm{talk}}), \tag{1}$$

where $P_{X\mathrm{talk}}$ is the crosstalk probability. Figure 2 shows the $\mathrm{ECF}_{X\mathrm{talk}}$ with red circles. It can be seen that it is the main source of correlated noise. It should be noted that the measurements are performed without the scintillator. A reflecting structure on the top of the SiPM can significantly increase the amount of optical crosstalk (Gola *et al* 2012b).

In scintillator based radiation detectors, the energy resolution that can be expressed as:

$$(\Delta E/E)^2 = 2.355 \times \left(\sigma_{\mathrm{intr}}^2 + \sigma_{\mathrm{stat}}^2 + \sigma_{\mathrm{el}}^2 + \sigma_{\mathrm{det}}^2\right), \tag{2}$$

where σ_{intr} is the intrinsic resolution of the crystal, σ_{stat} is the statistical contribution and σ_{el} and σ_{det} are related to the electronic and detector noise (i.e., dark counts), respectively. The noise related terms are often considered negligible at sufficiently high energies, such as 511 keV. The statistical contribution can be further modelled as:

$$\sigma_{\mathrm{stat}}^2 = (1/N_{\mathrm{scint}}) \times \mathrm{ENF}/(\mathrm{PDE} \times \epsilon), \tag{3}$$

where N_{scint} is the number of scintillation photons, ENF is the excess noise factor, PDE is the photodetection efficiency and ϵ is the light collection efficiency. If crosstalk is the only source of correlated noise, the ENF is equal to the ECF (Vinogradov *et al* 2009). For the afterpulse, on the other hand, the ECF is always higher than the ENF and the two values are equal at low gain only. Therefore, at a first approximation, the ECF can be considered an upper bound for the ENF.

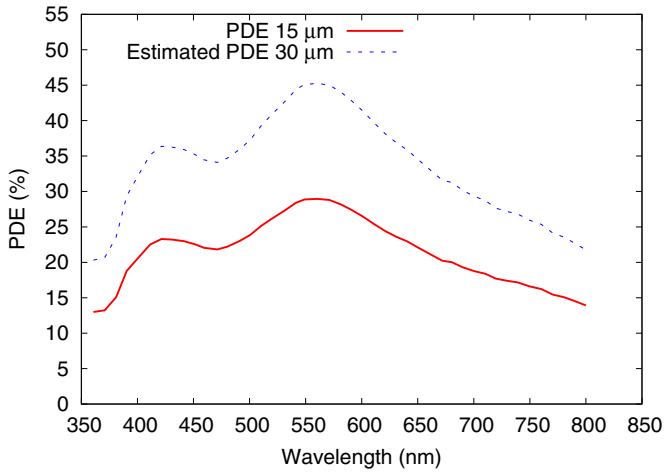

Figure 3. Measured PDE at 7.5 V OV as a function of wavelength for the 15 μm cell SiPM, and estimated for the 30 μm cell. Procedure described by Musienko *et al* (2006).

At 511 keV, the main contribution to the energy resolution is σ_{intr} since the large number of light photons produced by the gamma ray makes the statistical term almost negligible. As an example, a simple calculation using the LYSO light yield (32 ph keV^{-1}), an overall efficiency (PDE $\times$ ϵ) of 10%, and an ENF of 2 leads to a statistical contribution at 511 keV of 3.5%, whereas the intrinsic term is about 9%.

The PDE of the 30 μm cell SiPM was not measured directly. It has been estimated from the value of the 15 μm cell SiPM which has the same vertical structure (i.e. electric field), multiplying by the ratio of the nominal FFs. The result is presented in figure 3 (dashed line), showing a maximum expected PDE of 45% at 550 nm, well matching the GaGG emission, and 35% at 420 nm, which is the peak emission wavelength of LYSO.

The DCR was measured at -40 °C and extrapolated to 20 °C from its known temperature dependence (it doubles every $\sim$10 °C, Piemonte *et al* 2013). At 7 V OV it is about 4 MHz mm^{-2}. Accounting for the FF difference, the DCR of the first RGB-HD prototypes is a factor 4 higher than the RGB technology; this fact does not allow to reach full performance already at room temperature, as it will be discussed later on. The reason of the higher DCR is still under study: new production batches will clarify this point along with a process optimization.

3. SiPM characterization with scintillators

In this section, energy and timing resolution measurements for TOF-PET application with scintillators are presented. The tests were performed using 3 $\times$ 3 $\times$ 5 mm^3 crystals from Saint-Gobain (LYSO) and Furukawa (GaGG), wrapped in several layers of PTFE. The optical coupling with the detector was performed with a meltmount optical glue from 'Cargille Laboratories'. The detection units were irradiated with a ^{22}Na source that generates two photons at 511 keV and one at 1275 keV. The signal from the SiPM was first amplified by a 550 MHz bandwidth amplifier, and then digitized by an oscilloscope with 10 GS s^{-1} sampling rate and 1 GHz analogue bandwidth. No additional shaping was introduced before the digital conversion. The digital data were transferred to a PC in which a LabVIEW program performed the on-line analysis. All the analogue components (SiPM-crystal and fast amplifier)

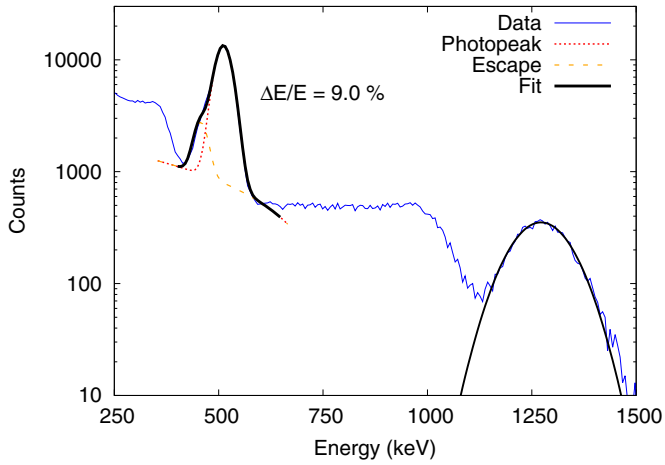

Figure 4. Energy spectrum obtained with the LYSO crystal at 8 V OV and −20 °C.

were placed inside a temperature controlled dark chamber. A detailed description of the measurement setup is given by Gola *et al* (2012a). Several SiPM samples have been tested to confirm the results.

The energy resolution measurements were performed with a single detection unit. The sampled signal was digitally integrated over an adjustable integration time (T_{int}). The resulting energy spectrum is always compressed because of the nonlinear response of the SiPM. Thus, a further analysis was performed to extract the energy resolution using the exponential saturation formula:

$$Q(E) = A \cdot [1 - \exp(-B \cdot E)], \tag{4}$$

where $Q(E)$ is the total charge delivered by the SiPM, E is the energy and A and B are two parameters determined imposing the ratio of the position of the two photopeaks to be the theoretical one (1275 keV/511 keV $\sim$ 2.5). Finally, the fit of the stretched 511 keV peak was calculated as the sum of two Gaussians (one for the photopeak and one for the escape peak relative to the K-edge of lutetium or gadolium), plus a linear background. The energy resolution was extracted as the ratio between the FWHM of the photopeak and its position.

The timing measurements were performed with two identical detection units irradiated with the ^{22}Na source placed head-on between them. Each SiPM was mounted on a double stage amplifier with two outputs. The first stage was used for the energy measurements while the other was used for timing. The energy channel allowed to select events in the 511 keV photopeak (full-width-at-tenth-maximum, FWTM). The timing channel included also a pole-zero (PZ) cancellation to reduce the baseline fluctuations determined by the pile-up of dark events (Gola *et al* 2013). No further digital signal processing in the analysis software was implemented before the leading edge discriminator. The acquisition program calculated the distance between the time pick off pairs at different threshold levels and created the corresponding histogram. A Gaussian fit was performed for each histogram and the CRT was extracted as its FWHM.

3.1. RGB-HD performance with LYSO

3.1.1. Energy resolution. The measurements of energy resolution with LYSO were performed with an integration time (T_{int}) of 400 ns (Gola *et al* 2012a). As an example, in figure 4 an energy spectrum obtained at −20 °C and 8 V OV is shown. The energy resolution at the 511 keV photopeak is 9.0% FWHM.

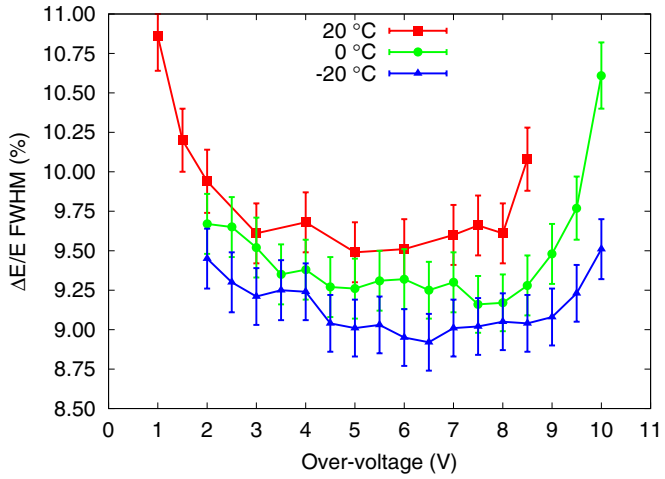

Figure 5. Energy resolution as a function of OV for LYSO and three temperatures.

The values for all the measured OVs and temperatures are shown in figure 5. In the low OV range, the PDE grows faster than the ENF with increasing OV thus, the statistical term of equations (2) and (3) decreases. This leads to an improvement of $\Delta E/E$ with bias. In the mid OV range, the statistical term becomes comparable to the intrinsic one. Furthermore, the PDE start saturating. These conditions lead to a flat region. The final deterioration at high OVs is caused by the fast increase of the ENF. Moreover, at higher OV, more dark counts can fall in the integrating window, possibly resulting in a performance degradation. The optimum is 9.5% FWHM at 20 °C in a range of OVs spanning from 5 to 8 V, and improves to 9.0% FWHM in an even wider bias range (from 4 to 9 V OV), at −20 °C. A lower temperature allows to reach slightly better results probably because of the improvement of the scintillation properties (the light yield increases with a rate of 0.2 %/°C, according to Mao *et al* 2011).

3.1.2. Timing resolution. Figure 6 shows an example of the CRT as a function of the threshold position along with the timing histogram of the optimum level (i.e., where minimum CRT is achieved). At −20 °C and 9 V OV, a CRT of 125 ps FWHM at a threshold level of 7 mV was obtained.

The optimal timing resolution with the LYSO crystal as a function of the OV and of the temperature is shown in figure 7. The combination of the high FF and high operating voltage allows the RGB-HD SiPM to reach CRTs comparable or even better than the values reported in literature: 157 ps FWHM at 20 °C, 138 ps FWHM at 0 °C and 125 ps FWHM at −20 °C. The improvement of the CRT with increasing OV is determined by the growth of the PDE. At 20 °C, the worsening at high OV is due to the DCR that produces signal baseline fluctuations not fully removed by the PZ filtering, nullifying the benefit of the higher PDE. The results are a substantial improvement compared to the previous FBK technology: about 30 ps at every temperature (Gola *et al* 2013).

3.2. RGB-HD performance with Ce:GaGG

3.2.1. Energy resolution. The energy resolution measurements with GaGG were performed with the same setup and procedure previously described for LYSO. With this new scintillator, different integration windows, from 200 ns to 2 μs, were used to find the best condition.

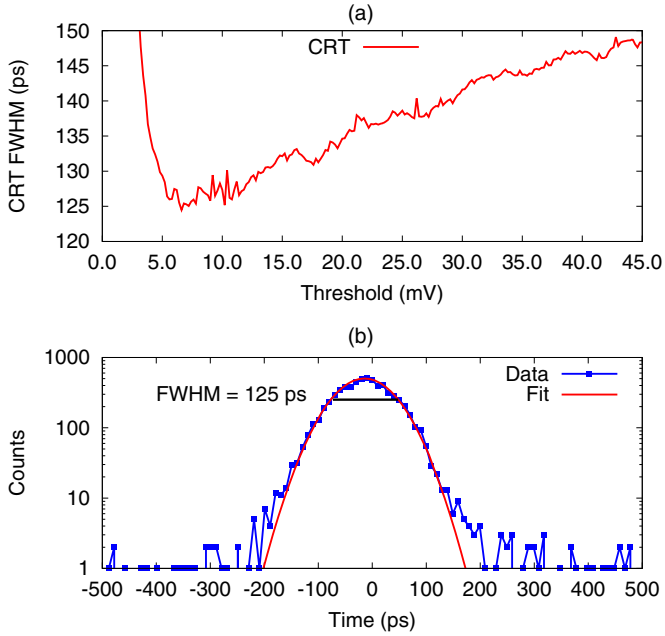

Figure 6. Example of the CRT as a function of the threshold (a) and timing histogram for the optimum threshold level. (b) Measurement conditions: −20 °C and 9 V OV.

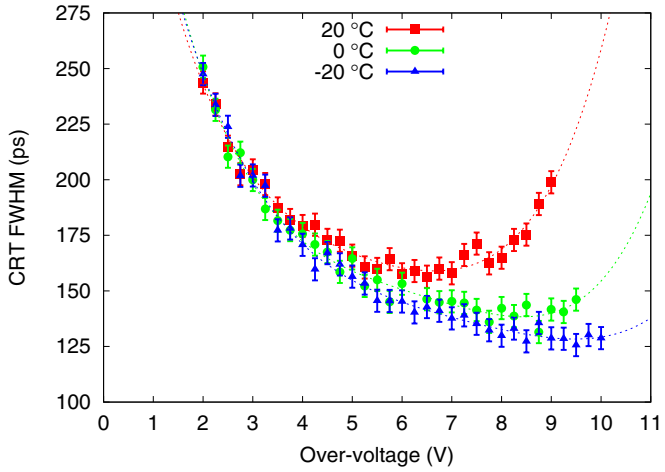

Figure 7. Timing resolution as a function of OV obtained with the LYSO crystal for the three temperatures. Polynomial fits are superimposed as a guide to the eye.

An example of the energy spectrum measured at 7 V OV and −20 °C with $T_{\text{int}} = 600$ ns is shown in figure 8. The energy resolution of the photopeak at 511 keV is 6.4% FWHM.

In figure 9, the dependence of the energy resolution on the integration time at −20 °C, for a subset of OVs, is plotted. In the low integration time range, the energy resolution has a decreasing trend because of the inclusion of an increasing part of the signal. Then, it

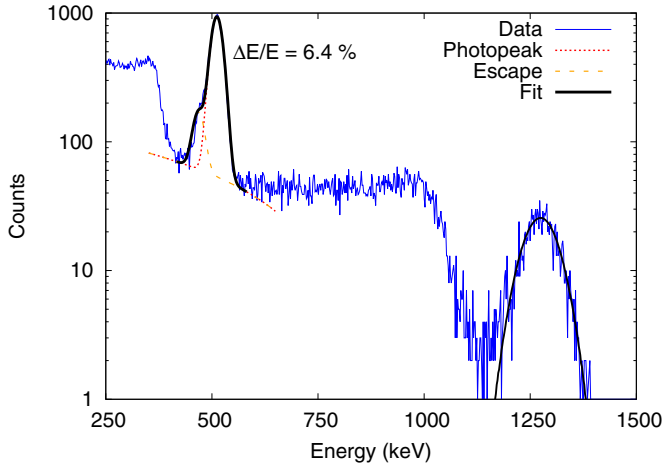

Figure 8. Example of energy spectrum for the GaGG crystal measured at −20 °C and 8 V OV with $T_{\text{int}} = 600$ ns.

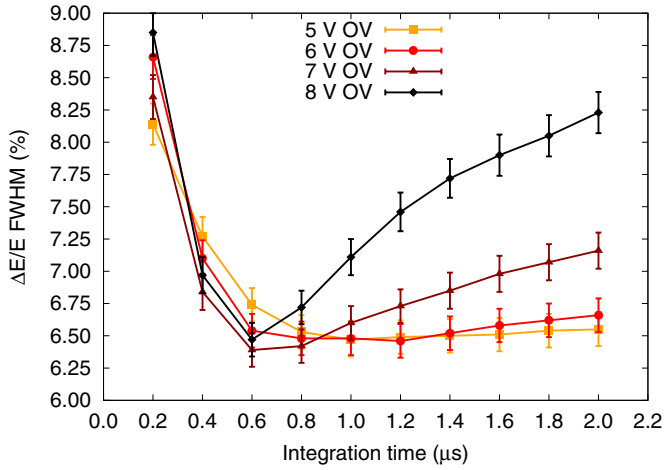

Figure 9. Energy resolution as a function of integration time for Ce:GaGG and four OVs. The temperature was set to −20 °C.

saturates and eventually slowly worsens because more noise (both primary and correlated) falls in the integration window. As the OV increases, since both the DCR and the ECF grow, the degradation of $\Delta E/E$ is steeper. Based on this, an optimum T_{int} of 600 ns was chosen. Figure 10 shows the measured energy resolutions as a function of the OV at the three temperatures. The best energy resolution is 7.0% FWHM at 20 °C and improves down to 6.4% FWHM at −20 °C. The optimum OV slightly increases from 6 V at 20 °C to 7 V at −20 °C. The high-density SiPM allows a slight improvement of the energy resolution w.r.t. RGB technology: about 0.3% at 20 °C (Kamada *et al* 2011). The gain is marginal because the intrinsic limit of about 6% at 511 keV and room temperature (Iwanowska *et al* 2013) dominates.

As expected, Ce:GaGG based detectors achieved better energy resolution than LYSO, due to the combination of: (i) higher light yield, (ii) emission wavelength closer to the maximum PDE of RGB-HD SiPMs and, most important, (iii) the lower crystal intrinsic energy resolution.

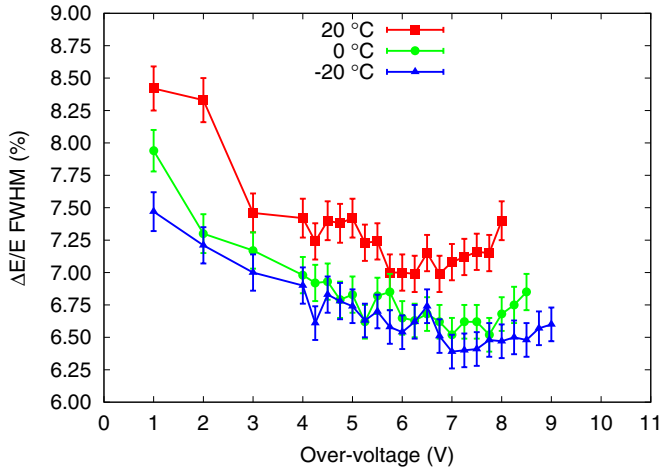

Figure 10. Energy resolution as a function of OV for Ce:GaGG at the three temperatures ($T_{\text{int}} = 600$ ns).

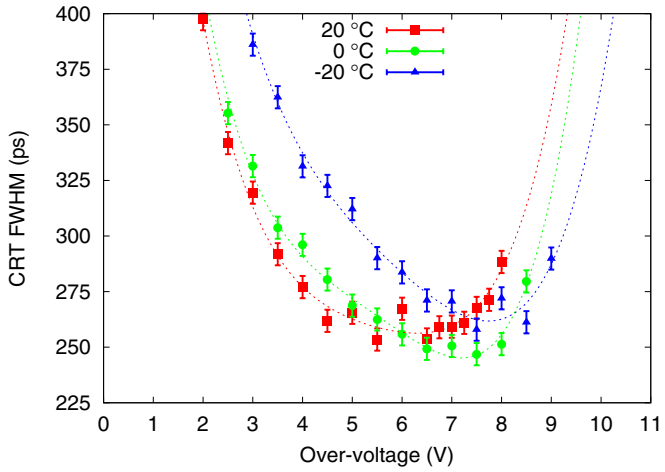

Figure 11. Timing resolution as a function of OV obtained with the GaGG crystal for the three temperatures. Polynomial fits are superimposed as a guide to the eye.

3.2.2. Timing resolution. The measurement procedure and the analysis of the optimum threshold level is the same previously described for LYSO. The CRT as a function of the OV obtained with the GaGG crystal is shown in figure 11. The measurements at 20 and 0 °C are very similar, with a minimum of 255 and 245 ps FWHM, respectively. The curve at −20 °C is higher in the low OV range but the best achieved value is only slightly worse (260 ps FWHM). The anomalous behaviour at −20 °C is probably related to the crystal because the SiPM performance improves with decreasing temperature, especially its noise. In fact, LYSO measurements show an improvement at low temperatures. Additional studies are ongoing to clarify the reasons of the deterioration at low temperatures.

The results represent an improvement of ∼30 ps w.r.t. RGB technology (Kamada *et al* 2011), and are almost a factor 2 better than what has been reported with PMTs and MPPCs (Iwanowska *et al* 2013, Yeom *et al* 2013b).

Table 2. Summary of measured energy and timing resolution with RGB-HD SiPMs, 4×4 mm^2, 30 μm CS. All reported values are FWHM.

		$\Delta E/E$ (%)		CRT (ps)	
Crystal	Size (mm^3)	20 °C	−20 °C	20 °C	−20 °C
Ce:LYSO	$3 \times 3 \times 5$	9.5 ± 0.2	9.0 ± 0.2	157 ± 5	125 ± 5
Ce:GaGG	$3 \times 3 \times 5$	7.0 ± 0.1	6.4 ± 0.1	255 ± 5	260 ± 5

3.3. Discussion

The best results of energy and timing resolution of the RGB-HD SiPMs coupled to Ce:LYSO and Ce:GaGG are summarized in table 2.

The energy resolution at 511 keV is lower with GaGG mainly because of its better crystal intrinsic term. At low temperature the resolution improves for both scintillators but the difference between the two materials remains constant (about 2.5%). On the other hand, the timing performance is better with LYSO because it represent the best compromise in terms of number of detected photons, and light emission rise and decay times (Seifert *et al* 2012c).

A second drawback of GaGG is the lower atomic number of its heavier element ($Z_{Gd} = 64$, compared to $Z_{Lu} = 71$). This translates into a lower probability of photoelectric interaction and, consequently, a higher measurement time needed to accumulate the same statistic in the 511 keV photopeak. For example, the measurements with GaGG shown in this paper required roughly a factor 2 more time than the ones with LYSO. Concerning the timing results presented here, it must be considered that a 4×4 mm^2 device has been used instead of the 3×3 mm^2 widely adopted in literature to characterize a SiPM technology. This makes the result even more relevant because the timing performance with a larger SiPM is degraded by the larger output capacitance and the higher DCR.

The combination of small cells and high FF of RGB-HD SiPMs leads to an improvement of the performance w.r.t. the RGB technology. This is due partly to the increased PDE and partly to the lower amount of correlated noise. The latter, in fact, affects both the energy resolution, by increasing the ENF, and the timing resolution, by strongly reducing the maximum operation voltage and thus the PDE (Gola *et al* 2012b).

4. Conclusions

In this paper, energy and timing resolution measurements for TOF-PET application with the newly developed FBK RGB-HD SiPM with 30 μm cells are shown. The developed technology features a high PDE with a lower amount of correlated noise (i.e., crosstalk and afterpulse). The performance evaluation was carried out with two scintillator crystals: Ce:LYSO and Ce:GaGG. With LYSO, RGB-HD SiPMs allowed to reach the state-of-the-art performance at 20 °C while improving it at −20 °C (9.0% FWHM $\Delta E/E$ and 125 ps FWHM CRT). The results have been obtained with a simple leading edge discriminator combined with pole zero filtering. Concerning GaGG, an energy resolution of 7.0% FWHM at 20 °C (which improves to 6.4% FWHM at −20 °C) was reported, while a coincidence timing resolution of 255 ps FWHM at 20 °C (with no relevant change with temperature) was shown. Both energy and timing resolutions represent an improvement of the state-of-the-art with this crystal.

Further activity is going on at the device level to increase the fill factor. Moreover, a comprehensive study on different cell sizes is in progress to find the best solution for the TOF-PET application.

Acknowledgments

The authors would like to thank I Musienko for performing and providing the photo-detection efficiency measurements shown in this paper. The research leading to these results has partially received funding from the European Union Seventh Framework [FP7/2007-2013] under grant agreement FP7-241711.

References

Gola A *et al* 2012a The DLED algorithm for timing measurements on large area SiPMs coupled to scintillators *IEEE Trans. Nucl. Sci.* **59** 358–65

Gola A *et al* 2012b SiPM cross-talk amplification due to scintillator crystal: effects on timing performance *IEEE Nucl. Sci. Symp. Med. Imaging Conf. Rec.* 421–3

Gola A *et al* 2013 Analog circuit for timing measurements with large area SiPMs coupled to LYSO crystals *IEEE Trans. Nucl. Sci.* **60** 1296–302

Haemisch Y *et al* 2012 Fully digital arrays of silicon photomultipliers (dSiPM) a scalable alternative to vacuum photomultiplier tubes (PMT) *Phys. Procedia* **37** 1546–60

Iwanowska J *et al* 2013 Performance of cerium-doped Gd3Al2Ga3O12 (GAGG:Ce) scintillator in gamma-ray spectrometry *Nucl. Instrum. Methods Phys. Res.* A **712** 34–40

Kamada K *et al* 2011 2-inch size single crystal growth and scintillation properties of new scintillator; Ce:Gd3Al2Ga3O12 *IEEE Nucl. Sci. Symp. Med. Imaging Conf.* 1927–9

Mao R *et al* 2011 LSO/LYSO crystals for future HEP experiments *J. Phys.: Conf. Ser.* **293** 012004

Musienko Y *et al* 2006 The gain, photon detection efficiency and excess noise factor of multi-pixel Geiger-mode avalanche photodiodes *Nucl. Instrum. Methods Phys. Res.* A **567** 57–61

Piemonte C *et al* 2012 Development of an automatic procedure for the characterization of silicon photomultipliers *IEEE Nucl. Sci. Symp. Med. Imaging Conf. Rec.* 428–32

Piemonte C *et al* 2013 Characterization of the first FBK high-density cell Silicon Photomultiplier technology *IEEE Trans. Electron Devices* **60** 2567–73

Saint-Gobain 2012 PreLude 420 datasheet (www.detectors.saint-gobain.com/PreLude420.aspx)

Seifert S *et al* 2012a Accurate measurement of the rise and decay times of fast scintillators with solid state photon counters *J. Instrum.* **7** P09004

Seifert S *et al* 2012b A comprehensive model to predict the timing resolution of SiPM-based scintillation detectors: theory and experimental validation *IEEE Trans. Nucl. Sci.* **59** 190–204

Seifert S *et al* 2012c The lower bound on the timing resolution of scintillation detectors *Phys. Med. Biol.* **57** 1797

Serra N *et al* 2013 Characterization of the new FBK SiPM technology for visible light detection *J. Instrum.* **8** P03019

Szczesniak T *et al* 2011 MPPC arrays in PET detectors with LSO and BGO scintillators *IEEE Nucl. Sci. Symp. Med. Imaging Conf. Rec.* pp 3272–8

Vinogradov S *et al* 2009 Probability distribution and noise factor of solid state photomultiplier signals with cross-talk and afterpulsing *IEEE Nucl. Sci. Symp. Med. Imaging Conf. Rec.* pp 1496–500

Yeom J *et al* 2013a Optimizing timing performance of silicon photomultiplier-based scintillation detectors *Phys. Med. Biol.* **58** 1207

Yeom J *et al* 2013b First performance results of Ce:GAGG scintillation crystals with silicon photomultipliers *IEEE Trans. Nucl. Sci.* **60** 988–92